Combined smoothing and decimation of complex pore network geometries

A.W.J. Heijs[1,2,5] , W.B.J.M. Janssen [3], C.P. Lowe [4,5], A.F. Bakker [5], R. Leenders [3]

[1] [2] e-mail: a.w.j.heijs@sc.dlo.nl ,
http://cpcoup5.tn.tudelft.nl/heijs/heijs.html ,
[1] Staring Centre for Integrated Land, Soil and Water Research (SC-DLO),Marijkeweg 11, 6700 AC Wageningen, The Netherlands, [2] Wageningen Agricultural University, Department of Soil Science and Geology, Duivendaal 10, 6700 AA Wageningen, The Netherlands.

[3] e-mail: wilfred@sara.nl , leenders@sara.nl , http://www.sara.nl/VC ,
SARA Visualization Center, Dutch Super computing Center Amsterdam, The Netherlands.

[4] e-mail: lowe@amolf.amolf.nl , http://cpcoup5.tn.tudelft.nl/lowe/lowe.html ,
FOM Institute for Atomic and Molecular Physics, Amsterdam, The Netherlands.

[5] e-mail: loek@cpcoup7.tn.tudelft.nl ,
http://cpcoup5.tn.tudelft.nl/bakker/bakker.html ,
Dept. of Computational Physics, Delft University of Technology, The Netherlands.

Abstract

A new approach to visualize local and global features of water patterns in complex pore networks in clay soils is presented. The pore network topology and water distribution in a soil sample were determined using computed tomography measurements and three-dimensional image processing techniques. The initial geometry of the pore contained too many triangles to visualize interactively. The pore geometry was smoothed and decimated in order to reduce the large number of triangles and improve the depth cue the isosurface. Local and global features were visualized using various techniques to allow better interpretations of the data.

1 Introduction and background

If one is interested in the transport of water and solutes in a soil, a natural starting point is the examination of the structure of pore networks. One can examine the spatial distribution of water in the soil and look for correlations between this water content distribution and the topology of the pore network. Determination of the occurrence of the large pores and the spatial variation of water content patterns are important for the study of preferential flow paths and distribution of nutrients or contaminants.

Once the structure of the soil sample is known, it can serve as a starting point for computer simulations of transport processes in a real porous medium, as opposed to the artificial model porous media frequently used [BRY92, BRY93]. The three-dimensional structure of pore networks is used for simulation of the flow velocity field in the pore. The relation between the geometry of the pore space and the flow field can be analyzed in terms of the occurrence of convective or diffusive flow patterns in typical regions of the pore space.

1.1 CT scanning

The first task is to determine the 3D pore space. A technique capable of producing, non-destructively, cross-sectional images of large pores (often called macro pores) and water patterns, with high spatial and contrast resolution, is computed tomography (CT). Although this technique is well-known in the field of medical imaging, it can also be used to scan dense objects such as a soil sample. A cilindrical clay soil sample was scanned along the axis which resulted in a stack of 146 adjacent CT slices of 512^2 pixels. The spatial resolution in the CT-images was 0.27 mm and the slice-thickness was 1 mm, resulting in a voxel size of $0.27 \cdot 0.27 \cdot 1.0$ mm. In an infiltration experiment we used a contrast agent (KI-solution) with a much higher CT-number than the CT-number of the clay soil. This resulted in a good contrast necessary for exact determination of the water distribution [HEI95a].

1.2 Image processing

To determine the topology of the pore networks in CT images of a dry cilindrical sample of a clay soil 3D image processing techniques were used [HEI96b]. Before image segmentation a 3×3 uniform filter per slice was used to remove noise, followed by Sobel filtering for edge enhancement. The image was segmented into regions of free space and solid material, based on the grey values in the original CT image. The bimodal grey value distribution of the object and background densities were approximated by two Gaussian distributions. A threshold value equal to the mean grey value of the pore network minus three standard deviations (of the pore network) was used. The high contrast between air in the pores and the clay background allowed a global thresholding for the segmentation whereby the connectivity and topology of the pore networks was conserved. After cluster analysis using 3D mathematical morphology we found 23 large connected clusters of voxels in the three-dimensional image of the macro pores, including one large continuous pore connecting top and bottom of the sample. This latter pore was used for further visualization. From the difference between the images of dry and wet samples the water distribution was determined. Different water contents were then visualized by simply thresholding the grey value image of the contrast agent [HEI95a, HEI96a].

2 Visualization of the pore network

The pore used for visualization consisted of almost 530 thousand voxels and a marching cubes algorithm was used to create an isosurface describing the contour of the pore [LOR87]. A threshold value of 0.5 was chosen. Binary voxels inside the pore were labelled 1, outside 0. The resulting isosurface consisted of over 575 thousand vertices and over 1.1 million triangles. This was clearly too much for interactive visualization and in order to render the isosurface in an acceptable time the number of triangles were reduced.

For correct visualization of the pore networks it is very important that the original topology of the pore structure is preserved as well as the size of the pore necks. When subsampling would be applied the topology of the pore is changed, i.e. parts of the pore that were not connected can become connected and create paths that are not really present in the sample. A better method to reduce the number of triangles in the isosurface

is described by Schroeder *et al.* [SCH92]. Their method, the decimation of triangle meshes, is very adequate for pore networks because the topology of the original network is preserved. Details on the decimation of the pore geometry are discussed below (see section 2.2).

2.1 Geometry smoothing

If an isosurface is produced with marching cubes from a data set with only two discrete values the surface will result in an irregular surface with lots of steps and corners, and the global shape of the pore structure is obscured by all these surface fluctuations and no good depth cueing is obtained. Furthermore, because of the sharp corners and abrupt surface changes decimation of the triangles in the surface will not be very efficient. We therefore decided to apply a geometric smoothing algorithm to the surface before triangle decimation.

In order to obtain a smoother surface with the same number of vertices and topology as the original surface a signal processing approach was used as described by G. Taubin [TAU94, TAU95]. This approach can be considered as a two-step filtering process. The first step is the application of a Gaussian filter to the vertex coordinates and the new coordinates are calculated by:

$$x_i' = x_i + \lambda \Delta x_i \tag{1}$$

Here x_i is the original position of vertex i, Δx_i is the average position of the nearest neighbors of vertex i, and λ is a positive scale factor. It is known that this method produces a shrinkage of the volume bounded by the isosurface. In order to compensate for this effect a second step is applied on the new coordinates.

$$x_i'' = x_i' + \mu \Delta x_i' \tag{2}$$

with $\mu < -\lambda$. Iterative application of these two steps results in a filter that can be characterized as a low-pass filter. The bandpass frequency, k_{bp}, of this filter can be calculated using:

$$k_{bp} = \frac{1}{\lambda} + \frac{1}{\mu} \tag{3}$$

The smoothing algorithm has three independent parameters that can be varied in order to achieve the best smoothing. Firstly, the pass-band frequency, k_{bp}, that determines the ratio between the global shapes and the features that will be smoothed away; secondly, λ which influences the amount of correction per iteration; and thirdly, the number of iterations that are applied to the original surface in order to obtain convergence.

We investigated the influence of variation of these parameters on the quality of the resulting geometry. If k_{bp} is too small features in the pore like thin tubes shrink too much and become threads and if λ is too small, convergence will be slow. On the other hand if k_{bp} is too large, the volume of the pore is not well preserved during smoothing. For the pore structure a smooth surface without significant volume changes was obtained in 100 iterations using $k_{bp} = 0.15$ and $\lambda = 0.25$. In figure 1 to 4 an original and smoothed detail of the pore structure are compared. The convergence of the smoothing algorithm is

shown in figure 5 by the average displacement per iteration cycle.

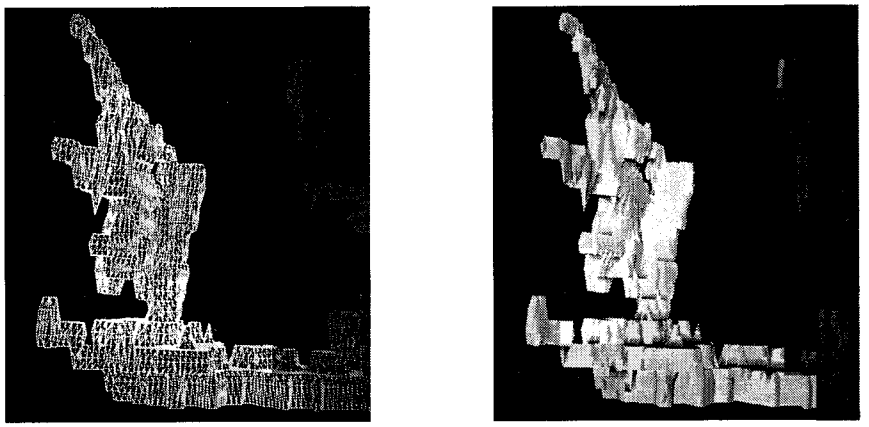

Figure 1: A part of the original pore structure.

Figure 2: A part of the original pore structure after it has been smoothed.

2.2 Triangle decimation

In the smoothing step the number of triangles in the surface is not changed, only the positions of the vertices are changed. In order to reduce the number of triangles to a workable level we applied the triangle decimation algorithm of Schroeder *et al.* [SCH92]. This algorithm checks all the vertices in the isosurface for possible removal. The criterion for removal is the distance of the vertex from the average plane formed by its neighboring vertices. If this distance is smaller than a chosen distance the vertex and its associated triangles are removed from the structure. The hole that is left by this removal is patched by a local retriangulation. This process can be repeated until convergence is reached.

The decimation algorithm can be separated into three steps. First the vertex is characterized according to its local geometry and topology. The type of the vertex determines whether it is a candidate for deletion or not. In this way it is possible to preserve certain

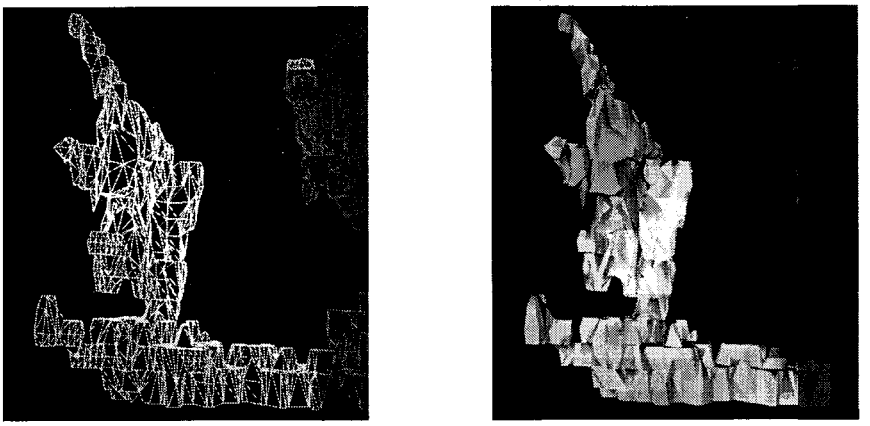

Figure 3: A part of the decimated pore structure.

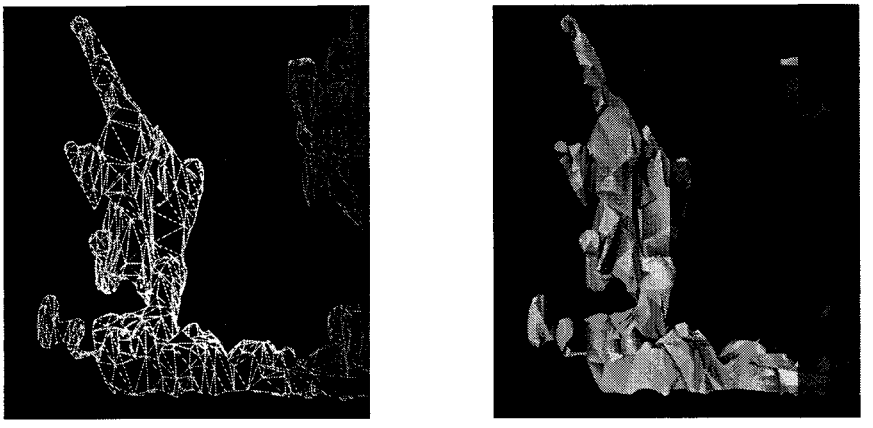

Figure 4: A part of the first smoothed and then decimated pore structure. At this value the reduction of the number of vertices is 77.3 % and the number of triangles is reduced by 77.6 %. After 10 iterations it consists of 130 thousand vertices and 255 thousand triangles.

features in the isosurface such as sharp edges and corners. After this characterization evaluation of the decimation criteria takes place. The average plane through the neighboring vertices is computed and the distance of the vertex to this plane is calculated. If this distance is smaller than the decimation parameter, the vertex and its associated triangles are removed. In the last step of the algorithm the hole is patched by retriangulation taking care that no duplicate triangles are generated. Also, the aspect ratio of the generated triangles is controlled so that acceptable triangles are produced.

First of all we investigated the influence of the decimation distance on the reduction of the number of triangles and the quality of the resulting surface. If the distance parameter is too small there will be no sufficient reduction, if it's too large the resemblance between the original surface and the resulting surface is lost. In figure 6 the reduction factor is plotted against the decimation parameter.

For this we used the isosurface that was obtained after smoothing as described in the

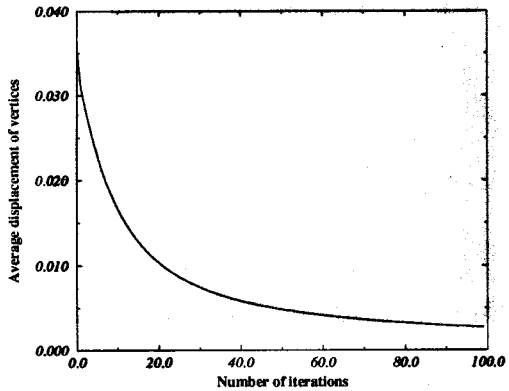

Figure 5: Convergence of the smoothing algorithm.

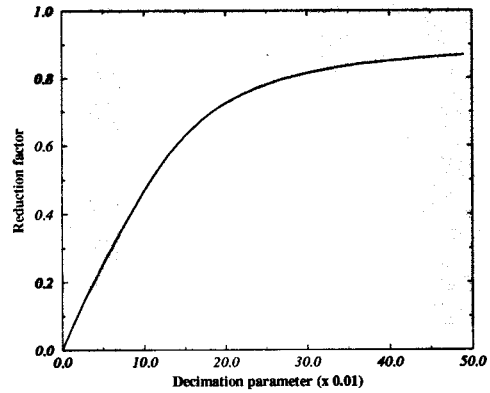

Figure 6: Reduction of polygons as a function of the decimation parameter.

previous section. From figure 6 we see that for small values of the decimation parameter the reduction increases fast. This means that there are a lot of vertices in (almost) flat regions of the isosurface that can be removed. If the decimation parameter increases over 0.2, hardly any increase in the reduction factor is achieved. This points out that beyond this point vertices can only be removed at the cost of significant changes in the surface geometry and we concluded that for our pore structure the best decimation parameter is 0.2. At this value the reduction of the number of triangles is 77.6 % which is reached in 10 iterations. The origal (left) and resulting pore surface (right) are shown in figure 7.

In order to demonstrate the effect of smoothing the surface the original unsmoothed surface was decimated. As expected the performance of the decimation algorithm is worse in this case because of the irregular surface. With a decimation parameter of 0.2 the reduction in the number of vertices is only 58.8 %. In figure 1 to 4 a detail of the pore is shown after decimation and after smoothing and decimation.

2.3 Visualization of water content patterns

Although isovalue surfaces for water content and pore space provide a better depth cue, it is not possible to present the complex pore space topology with all it's geometrical information in a single visualization, since many branching pores themselves are contained within an isovalue surface of the water content distribution. Visualizing these isovalue surfaces transparently results in several successive transparent surfaces, making it more difficult to interpret such a visualization.

Another approach is to use 2D texture mapping to remove convex surface regions [TES95], whereas the rest of the surface can be color-coded according to the water content to visualize the wetting of the pore surfaces. The disadvantage that large parts of the global structure of the pore network will become invisible, making interpretation of the visualized data more complex. When there is enough symmetry in the pore structure one can create a "cut-away-view" to visualize inner water content isosurfaces with different transparency values, but normally this is not possible due to the irregular complex

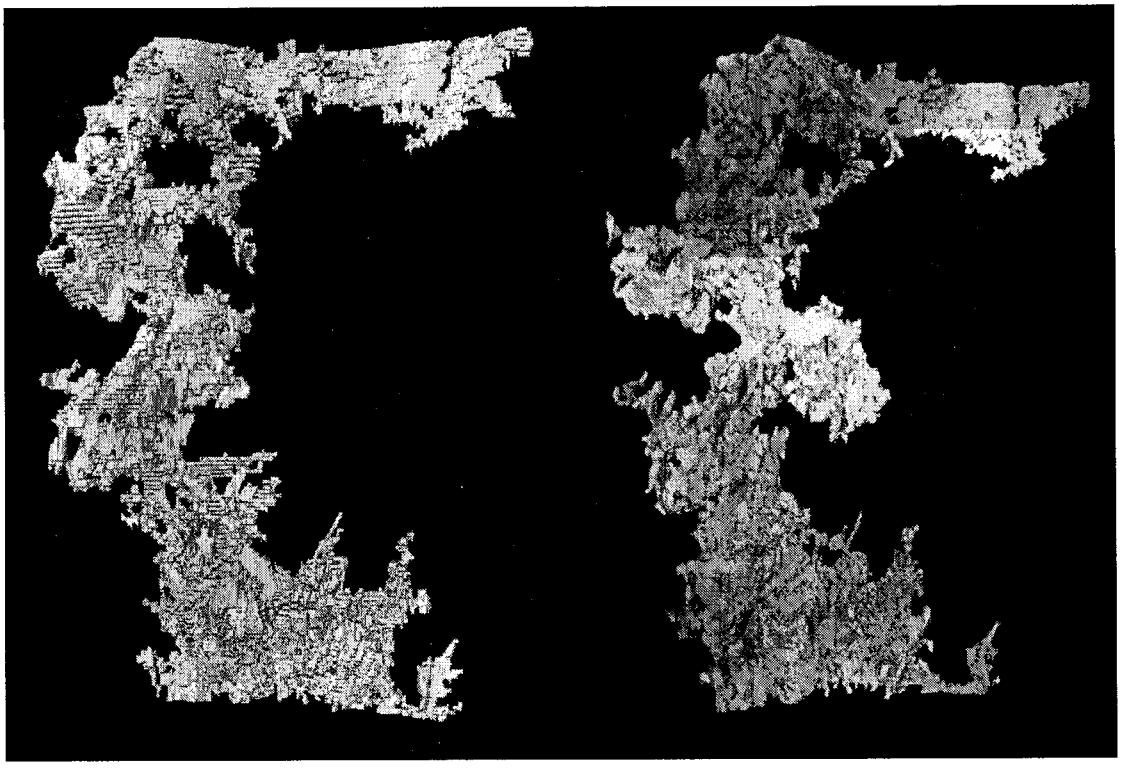

Figure 7: The original isovalue surface (left) and the smoothed and decimated isovalue surface (right) of the total pore network geometry.

structure of porous media.

Visualizing flow behavior in complex topologies, like pore networks with many branchings and closed loops is very difficult since parts of the pore network obscure other parts independent of the viewing angle. Which part of the pore network is the main flow path and how is the flow field influenced by branchings are questions which involve the total structure of the pore network as well as the local shape. These global and local features of the flow field are difficult to analyze.

By color-mapping the pore surface using the whole range of water content values, a strong spatial correlation between these water content patterns and the preferential flow path in the large pore-network was found [HEI96a]. It was also found that the flow paths at the macro pore scale are strongly correlated with the geometrical structure of the macro pore network, especially for water content values lower than 20 % (expressed as a percentage by volume). The visualizations also show water content patterns which are largely gravity driven, with the small degree of lateral spreading, characteristic of fingered flow [HEI96a].

2.4 Visualization of the velocity field

Most porous media of practical interest have extremely complex 3D geometries. However, the 3D CT images gave us the opportunity to study them in detail, using computer simulation to calculate the flow in such media. We used a lattice Boltzmann technique to solve the Navier-Stokes equations for the flow in the complex pore network [HEI95b]. The details of this approach are well documented [LAD94a, LAD94b]. In order to perform the calculations a map of free space and solid matrix is needed from which to compile a list of boundary links. For the soil sample the solid/matrix map is directly read from a segmented CT image. Having determined the steady-state velocity field for a given pressure gradient yields the mean flow velocity field directly. Applying Darcy's law the permeability of the clay soil was calculated and compared very well with experimental values [HEI95b].

A good depth cue is important for the interpretation of the velocity flow field inside a complex pore network with many small branches and the visual analysis of the relationship between the pore geometry and the principal path by which the fluid flows through the pore network. We found that in areas of the pore which lie away from this path there is very little flow, and even upward flow [HEI95b]. The velocity field itself was coarsely averaged, leaving enough vectors to give a strong impression of the flow, but not so many that the flow in more central regions was obscured by peripheral vectors.

Future work will focus on using the geometric pore structure information in extensive numerical flow pattern simulations, that will be compared with the observed water distributions. It is shown that visualization of the highly irregular pore structure reveals detailed knowledge which could not be obtained otherwise. Furthermore, the visualizations presented in this work are essential in judging the correlation between the experimental and numerical approaches. An animated flight through the pore space will also enable us to examine in detail the flow environment experienced by a convecting solute particle; a detailed visualization of the flow patterns in the lateral parts of the pore should shed light on the mechanisms of 'hold up' dispersion.

3 Conclusions

In this article a clay soil sample is examined in large detail. From computed tomography images we reconstructed a pore network that consisted of over 500,000 voxels.The isosurfaces created contained a similar number of triangles, which is rather large for interactive visualization. It was therefore decided to reduce the number of triangles in such a way that almost no information is lost. Subsampling obviously is inadequate for this purpose. Decimation, however, is known to reduce the number of triangles without changing local and global features too much. In this work we show that for the 'high-frequency' isosurface it is very helpful to first smooth the isosurface before applying decimation. This results in, visually judged, higher quality geometries than obtained with decimation alone.

From the CT measurements of the 'wetted' clay soil samples information about local water content could be combined to obtain water content patterns. The combination of the pore structure and the water distribution in one visualization contributes greatly to the understanding of the relation between both features.

4 Acknowledgments

This research is financed by the Dutch Agricultural Research Department (DLO-NL) and partly by the 'Nederlandse Organisatie voor Wetenschappelijk Onderzoek' (NWO).

References

[BRY92] S.L. Bryant and M. Blunt, *Phys. Rev.* **A46**:2004 1992.

[BRY93] S.L. Bryant, P.R. King and D.W. Mellor, *Transport in Porous Media* **11**:53, 1993.

[HEI95a] A.W.J. Heijs, J. de Lange, J.F.Th. Schoute and J. Bouma, *Computed tomography as a tool for non-destructive analysis of flow patterns in macroporous clay soils.* Geoderma. 65: 1-19, 1995.

[HEI95b] A.W.J. Heijs, and C.P. Lowe, *Numerical evaluation of the permeability and the kozeny constant for two types of porous medium.* Physical Review E, Vol. 51 No. 5: 4346-4352, 1995.

[HEI96a] A.W.J. Heijs, C.J. Ritsema and L. W. Dekker, *Three-dimensional visualization of preferential flow patterns at different scales.* Geoderma, 70:101–116, 1996.

[HEI96b] A.W.J. Heijs and J. de Lange, *Determination of 3D pore networks and water content distributions from CT-images.* To be submitted to: BioImaging.

[LAD94a] A.J.C. Ladd, *J. Fluid Mech.* **271**:285 1994.

[LAD94b] A.J.C. Ladd, *J. Fluid Mech.* **271**:311 1994.

[LOR87] W. Lorensen and H. Cline, *Marching cubes: A high resolution 3d surface construction algorithm.* Computer Graphics (Proceedings SIGGRAPH'87), 163–169, 1987.

[SCH92] W.J. Schroeder, A. Zarge, and W.E. Lorensen, *Decimation of triangle meshes* Computer Graphics (Proceedings SIGGRAPH'92), 26: 65–70, 1992.

[TAU94] G. Taubin, *Curve and surface smoothing without shrinkage.* Technical Report RC-19536, IBM Research, April 1994.

[TAU95] G. Taubin, *A signal processing approach to fair surface design.* Computer Graphics (Proceedings SIGGRAPH'95), 351–358, 1995.

[TES95] M. Teschner and C. Henn, *Texture mapping in technical, scientific and engineering visualization.* SGI internal report, April 24, 1995.